Communication

Ag–Au–Ag Heterometallic Nanorods Formed through Directed Anisotropic Growth

Daeha Seo, Choong Il Yoo, Jongwook Jung, and Hyunjoon Song

J. Am. Chem. Soc., **2008**, 130 (10), 2940-2941 • DOI: 10.1021/ja711093j

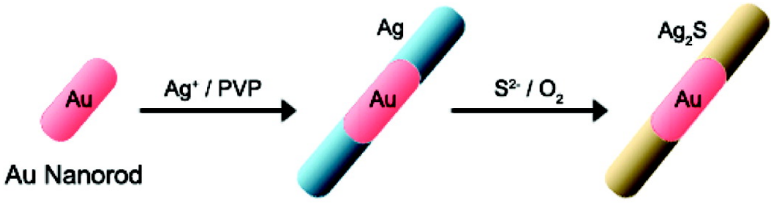

More About This Article

Additional resources and features associated with this article are available within the HTML version:

- Supporting Information
- Links to the 5 articles that cite this article, as of the time of this article download
- Access to high resolution figures
- Links to articles and content related to this article
- Copyright permission to reproduce figures and/or text from this article

View the Full Text HTML

J|A|C|S
COMMUNICATIONS

Published on Web 02/19/2008

Ag−Au−Ag Heterometallic Nanorods Formed through Directed Anisotropic Growth

Daeha Seo, Choong Il Yoo, Jongwook Jung, and Hyunjoon Song*

Department of Chemistry and School of Molecular Science (BK21), Korea Advanced Institute of Science and Technology, Daejeon 305-701, Korea

Received December 18, 2007; E-mail: hsong@kaist.ac.kr

Heterostructured nanocrystals containing multiple components are attracting attention due to not only their multifunctional properties but also new features arising from the effective coupling of different domains.[1,2] Numerous semiconducting heterostructures have been synthesized by gas-phase deposition and are being used for the miniaturization of electronic and photonic circuits.[3] Metallic heterostructures, in contrast, are generally grown on hard templates such as anodic aluminum oxides by electrochemical deposition.[1,4] Synthesis without templates is relatively difficult owing to distinct reduction rates and lattice mismatch of the different components. Even when selecting materials with similar lattice constants, precise tuning of the reaction conditions is strictly required for the formation of multimetallic nanostructures. Xu et al. successfully generated heterodimer particles at a micelle liquid−liquid interface,[5] and Yang et al. utilized polyhedral Pt nanocrystals to induce either isotropic growth of Pd nanopolyhedrons epitaxially or anisotropic growth of Au nanowires heterogeneously.[6] There have been few reports of the synthesis of multisegmented metallic nanostructures without hard templates despite the fact that this approach is advantageous in terms of structural variety and controllability.

We have recently demonstrated that single-crystalline polyhedral gold nanocrystals such as cubes, cuboctahedrons, and octahedrons could be readily formed by the preferential overgrowth of spherical particles.[7] Using a similar strategy, we promoted anisotropic growth from multiply twinned particles (MTPs). In the present work, we report the synthesis of Ag−Au−Ag heterometallic nanorods through directed overgrowth from gold decahedrons and rods by adding silver ions and poly(vinyl pyrrolidone) (PVP) (Figure 1a). The silver component was readily converted to Ag_2S by reaction with Na_2S to generate a semiconductor−metal−semiconductor heterojunction on the nanorods.

Briefly, multiply twinned gold decahedrons were used as a seed.[8] The particle dispersion in diethylene glycol (DEG) was heated to the boiling temperature (260 °C), and 2 equiv of silver nitrate with respect to the gold concentration and PVP solutions in DEG were added periodically into the dispersion every 30 s over a period of 7.5 min. Refluxing the reaction mixture for 1 h yielded new nanorods in a high yield. As shown in the scanning electron microscopy (SEM) image in Figure 1b, each nanorod has a bright strip on the center, indicating that a heterometallic component with high reflectivity (Au) is included in the structure. The nanorods are estimated to be 194 ± 17 nm in length and 76 ± 9 nm in diameter, and the average aspect ratio is 2.6 ± 0.5. For an accurate structural analysis, gold nanorods with a 5-fold symmetry were used for the reaction. After the periodic addition of $AgNO_3$ and PVP solutions, longer nanorods were formed in a high yield. Figure 1c exhibits nanorods with a thick bright strip on the center, indicating that the silver segments were grown symmetrically at both ends of the original gold nanorods. The average size of the product is estimated to be 440 ± 40 nm in length and 100 ± 11 nm in diameter

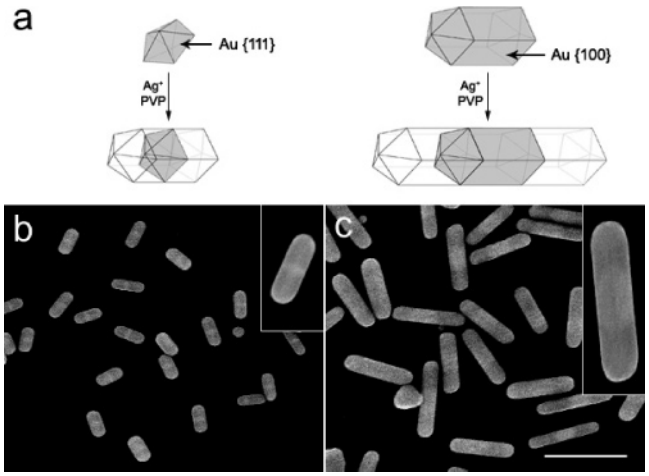

Figure 1. (a) Synthesis of Ag−Au−Au heterometallic nanorods from gold decahedrons and rods. SEM images of Ag−Au−Ag heterometallic nanorods grown from (b) gold decahedrons and (c) rods. The bar represents 500 nm.

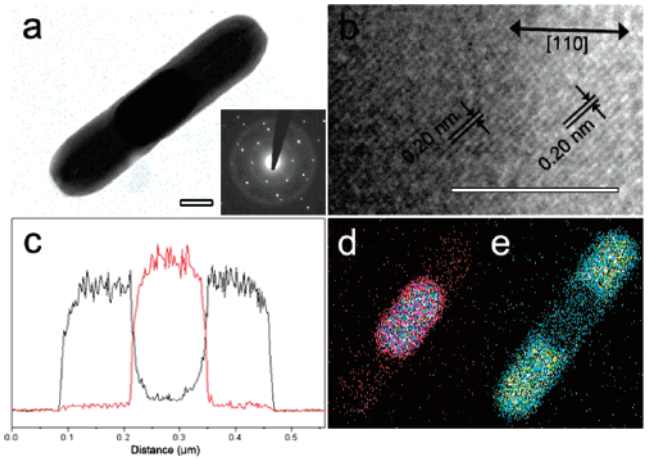

Figure 2. (a) TEM image and SAED pattern of a single Ag−Au−Ag nanorod; (b) HRTEM image of a nanorod at the boundary of gold and silver; (c) line profile analysis of silver (black) and gold (red) along the long axis of a nanorod; elemental mapping of gold (d) and silver (e). The bars represent 50 nm (a) and 2 nm (b).

with an average aspect ratio of 4.5 ± 0.7. The gold and silver segments in a nanorod are clearly distinguished in the transmission electron microscopy (TEM) image (Figure 2a). The average length (194 ± 24 nm) and diameter (93 ± 3 nm) of the gold segments are nearly unchanged from those of the original seeds after the silver overgrowth. The gold nanorods were successfully regenerated by selective dissolution of silver components with HNO_3, and there was no indication of Ag−Au alloy formation in the interface (Figure S2 in Supporting Information). The selected area electron diffraction (SAED) exhibits a superposition of the diffractions along ⟨111⟩ and

10.1021/ja711093j CCC: $40.75

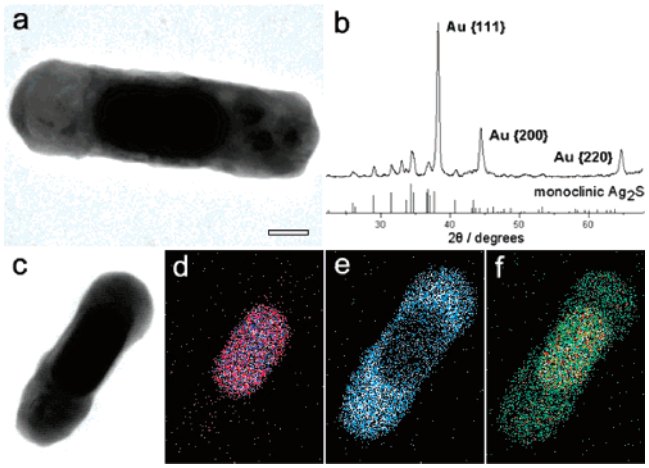

Figure 3. (a) TEM image and (b) XRD pattern of $Ag_2S-Au-Ag_2S$ nanorods; (c) scanning TEM image and elemental mapping of gold at 2.120 keV (d), silver at 2.984 keV (e), and both gold and sulfur at 2.307 keV (f). The bar represents 50 nm.

⟨100⟩ zone axes in a face centered cubic lattice.[9] The clear spots of the SAED pattern and continuous lattice fringe images at the gold−silver junction strongly support that the silver segments are grown epitaxially on the gold nanorod surface. The lattice spacings between neighboring fringes in gold and silver regions are 0.20 nm, corresponding to the distance between two adjacent {200} crystallographic planes. The growth direction of the rod is [110] as indicated in Figure 2b. The line profile of the composition along the long axis of the nanorods in Figure 2c shows clear boundaries of Ag, Au, and Ag segments with an intensity ratio of 1:1:1. Elemental mapping of silver and gold (Figure 2d,e) also reveals a multisegmented feature of the Ag−Au−Ag nanorod. The X-ray photoelectron spectrum of the rods (Figure S4) exhibits Ag 3d and Au 4f bands, indicating that both segments are exposed on the surface.

Several groups have proposed a growth mechanism for metal nanorods.[10] In our experiment, nanorods were directly grown from well-defined multiply twinned decahedral particles, providing direct insight into the general mechanism. The silver deposition on the decahedral seeds led to the formation of high-energy surfaces such as {100} and {110}, where PVP binds more efficiently than on the {111} surface. Consequently, silver segments were grown fast along the longitudinal direction of the nanorods, but slow along the lateral direction, due to PVP blocking of the high-energy surfaces. In this mechanism, the three-dimensional decahedral structure of the seeds is detrimental to guiding anisotropic growth directions. Empirically, only irregular round particles were obtained by adding silver precursor and PVP in the absence of gold decahedral seeds (Figure S5). This mechanism is consistent with that of silver nanowire formation proposed by Xia et al.[11]

Each segment of the Ag−Au−Ag nanorods has a distinct chemical property. Silver readily forms oxides and sulfides, but gold is stable at ambient temperature. By the addition of Na_2S to the nanorods in water, silver segments were converted to silver sulfide stoichiometrically. Figure 3a shows that the entire rod structure is preserved despite that large sulfur anions are introduced into the lattice. X-ray diffraction (XRD) data (Figure 3b) reveal that monoclinic Ag_2S (JCPDS 14-0072) are generated. The atomic ratio of Ag/S is calculated to be 2:1 in the energy dispersive X-ray spectrum (EDS) (Figure S6), and a high-resolution TEM (HRTEM) image shows polycrystalline lattice fringes of the silver sulfide domain (Figure S7). Elemental mapping of Au and Ag (Figure 3d,e) shows the confinement of each component in different regions. Mapping at 2.307 keV covers all domains of the rod, because of the partial overlap between S Kα and Au Mα peaks. The UV−vis spectrum of $Ag_2S-Au-Ag_2S$ nanorods exhibits a broad peak centered at 700 nm (Figure S9), where such a large red-shift from that of the Ag−Au−Ag nanorods is due to the high refractive index of silver sulfide.[12]

In conclusion, Ag−Au−Ag heterometallic nanorods were synthesized by directed anisotropic growth from multiply twinned gold decahedrons and rods. $Ag_2S-Au-Ag_2S$ heterojunctions were generated in the nanorods by reaction with sulfide ions. This template-free synthesis may be generalized to other metal and metal oxide systems for electronic, sensing, and catalytic applications.

Acknowledgment. This work was supported by the Nano R&D Program 2007-02668 and a grant from the Korea Science and Engineering Foundation (KOSEF), funded by the Korean Government (MOST) (Grant No. R11-2007-050-04002-0).

Supporting Information Available: Detailed experimental procedures, size distribution histograms, EDS, line profiles, and XPS spectra of Ag−Au−Ag nanorods and a HRTEM image, EDS, line profiles, and UV−vis spectrum of $Ag_2S-Au-Ag_2S$ nanorods. This material is available free of charge via the Internet at http://pubs.acs.org.

References

(1) Hurst, S. J.; Payne, E. K.; Qin, L.; Mirkin, C. A. *Angew. Chem., Int. Ed.* **2006**, *45*, 2672.
(2) (a) Milliron, D. J.; Hughes, S. M.; Cui, Y.; Manna, L.; Li, J.; Wang, L.-W.; Alivisatos, A. P. *Nature* **2004**, *430*, 190. (b) Taleb, M.; Rothenberg, E.; Popov, I.; Costi, R.; Banin, U. *Science* **2004**, *304*, 1787.
(3) (a) Wu, Y.; Fan, R.; Yang, P. *Nano Lett.* **2002**, *2*, 83. (b) Gudiksen, M. S.; Lauhon, L. J.; Wang, J.; Smith, D. C.; Lieber, C. M. *Nature* **2002**, *415*, 617. (c) Lauhon, L. J.; Gudiksen, M. S.; Wang, D.; Lieber, C. M. *Nature* **2002**, *420*, 57.
(4) Nicewarner-Peña, S. R.; Freeman, R. G.; Reiss, B. D.; He, L.; Peña, D. J.; Walton, I. D.; Cromer, R.; Keating, C. D.; Natan, M. J. *Science* **2001**, *294*, 137.
(5) Gu, H.; Zheng, R.; Zhang, X.; Xu, B. *J. Am. Chem. Soc.* **2004**, *126*, 5664.
(6) Habas, S. E.; Lee, H.; Radmilovic, V.; Somorjai, G. A.; Yang, P. *Nature Mater.* **2007**, *6*, 692.
(7) (a) Seo, D.; Yoo, C. I.; Park, J. C.; Park, S. M.; Ryu, S.; Song, H. *Angew. Chem., Int. Ed.* **2008**, *47*, 763. (b) Seo, D.; Park, J. C.; Song, H. *J. Am. Chem. Soc.* **2006**, *128*, 14863.
(8) Seo, D.; Yoo, C. I.; Chung, I. S.; Park, S. M.; Ryu, S.; Song, H. *J. Phys. Chem. C* **2008**, *112*, 2469.
(9) (a) Johnson, C. J.; Dujardin, E.; Davis, S. A.; Murphy, C. J.; Mann, S. *J. Mater. Chem.* **2002**, *12*, 1765. (b) Lisiecki, I.; Filankembo, A.; Sack-Kongehl, H.; Weiss, K.; Pileni, M.-P.; Urban, J. *Phys. Rev. B* **2000**, *61*, 4968.
(10) (a) Liu, M.; Guyot-Sionnest, P. *J. Phys. Chem. B* **2005**, *109*, 22192. (b) Murphy, C. J.; Sau, T. K.; Gole, A. M.; Orendorff, C. J.; Gao, J.; Gou, L.; Hunyadi, S. E.; Li, T. *J. Phys. Chem. B* **2005**, *109*, 13857. (c) Wei, Z.; Zamborini, F. P. *Langmuir* **2004**, *20*, 11301.
(11) Sun, Y.; Mayers, B.; Herricks, T.; Xia, Y. *Nano Lett.* **2003**, *3*, 955.
(12) Liu, M.; Guyot-Sionnest, P. *J. Mater. Chem.* **2006**, *16*, 3942.

JA711093J